MODELING OF THE MATERIAL PROPERTIES AND FLUID-STRUCTURE INTERACTION IN THE TRAUMATIC RUPTURE OF AORTA

Sang-Hyun Lee
Kurosh Darvish
Center for Applied Biomechanics
University of Virginia
United States
Libor Lobovsky
Department of Mechanics
University of West Bohemia
Czech Republic
Paper Number 05-0390

ABSTRACT

Traumatic rupture of the aorta (TRA) is a leading cause of fatality in motor vehicle crashes. However, its injury mechanisms are still unknown since it is difficult to replicate and evaluate such ruptures experimentally. In this study, the mechanisms of aortic rupture in dynamic pressure loading were investigated using Finite Element (FE) Analysis.

A hyperelastic material model with linear viscoelasticity was used to characterize the mechanical behavior of aorta based on oscillatory biaxial tests and literature data. It was shown that the previous data led to contradictory uniaxial and biaxial responses. A set of new material properties were identified which closely described all the available experimental data.

Furthermore, a Finite Element model of aortic arch was studied under pressure impulse as seen in cadaveric sled tests. Four approaches were used to model the fluid namely, Lagrangian, Eulerian, Arbitrary Lagrangian-Eulerian (ALE), and Smoothed Particle Hydrodynamics (SPH). The Eulerian approach, in which the mesh is fixed in space through which the material flows, was the most complete one in terms of modeling the flow and interaction with the wall, though it required relatively large computational time. In the ALE approach, a Lagrangian material deformation was considered followed by an advection cycle for smoothing the mesh. The result of the ALE approach compared to the Eulerian approach showed less flow and localized deformation. In the SPH formulation, the fluid was represented by particles which interact with one another and the surroundings through specific potential energy functions. The SPH approach exhibited rather idealized behavior of the fluid flow with less computational time. The TRA models were validated against *in vitro* tests and predicted the most probable location of rupture at the isthmus as indicated in the experiments.

INTRODUCTION

Traumatic rupture of the aorta (TRA) is a major cause of fatality in automobile accidents. According to the previous studies, aortic injuries continue to be present in about 20 percent of motor vehicle crash fatalities [1, 2]. The injury mechanism of TRA is still unknown and it is difficult to replicate and evaluate such ruptures experimentally, though different hypotheses have been proposed. The TRA due to pressure was the focus of this study. Other proposed mechanisms of TRA include relative motions and osseous pinching [3, 4]. The primary site of the TRA is reported at the isthmus region with the probability of 75-85%, which is the transition between a relatively mobile heart and a relatively fixed descending aorta [1, 5].

Before failure aorta undergo large deformations due to the internal pressure, the inertial forces, and the contact forces acting upon aorta from the surrounding tissues. Simulation of aorta in impact loading using finite element (FE) analysis was conducted to improve the understanding of the mechanisms of aortic injury. The biofidelity of the results of the FE model is in part dependent on the choice of material constitutive model. The uniaxial and biaxial experimental data of Mohan and Melvin (MM) showed that the mechanical behavior of aorta is rate dependent and failure occurs at stretch ratios more than 60% [6, 7]. Previous FE studies simplified aortic blood with linear elastic fluid model which is incapable of sustaining large deformations [8, 9]. Complicated and more realistic flow interaction with the aortic wall can be accomplished by applying such techniques as Arbitrary Lagrangian Eulerian method (ALE) or Smoothed Particle Hydrodynamics (SPH).

METHODS

Material Model

A representative rectangular piece (20.5 mm x 18.4 mm x 1.36 mm) of human aorta, sample HA41, was subjected to biaxial oscillatory stretch at 20 Hz superimposed on a constant stretch, using the test setup described in [10] (Figure 1). The sample was excised from the arch of aorta of a 27 year-old subject and was connected to two shakers and two load cells using 12 silk sutures. The oscillatory deformation was determined based on the measured accelerations of the two shakers moving in the circumferential and longitudinal directions. The biaxial forces were measured using two load cells mounted opposite to the shakers. The displacement offsets and the time history of the state of strain in the central quadrilateral region, PQRS, were determined based on motion analysis of high speed (1000 frames/sec) video photography of the sample deformation.

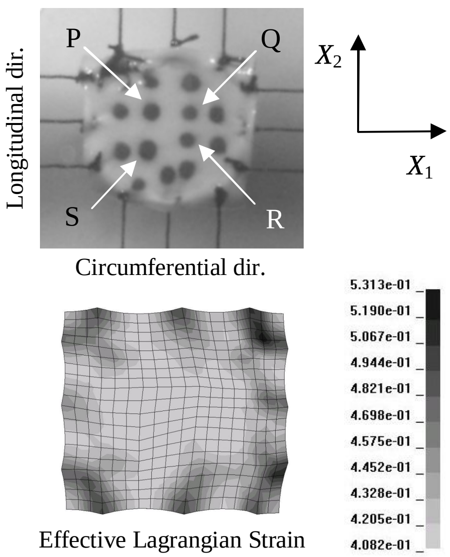

Figure 1. HA41 aorta sample and its FE model for biaxial testing at 20Hz

A second-order Mooney-Rivlin (MR) constitutive model of the following form, for an isotropic material, was assumed for aorta:

$$W = C_{10}(I_1 - 3) + C_{01}(I_2 - 3) + C_{11}(I_1 - 3)(I_2 - 3) + C_{20}(I_1 - 3)^2 + C_{02}(I_2 - 3)^2 \quad (1)$$

in which, W is the strain energy function, C_{ij} are the material properties and I_i are the invariants of the left Cauchy-Green strain tensor. The above equation is compatible with material 77 in LS-DYNA [11]. Viscoelasticity of the material was approximated by adding a one-term Prony series, $G(t)=2m_0\exp(-bt)$, to the hyperelastic shear modulus, where $m_0=2(C_{10}+C_{01})$ is the linear shear modulus and b is the decay rate. The factor 2 in $G(t)$ was chosen based on the ratio between the dynamic and quasi-static result given in [6]. The hyperelastic material properties were determined by least-squares optimization of an analytical solution for the biaxial forces subject to a general biaxial deformation. The viscoelastic decay rate was determined based on the phase shifts between the oscillatory displacements and forces. For the quasi-static and dynamic uniaxial test data (MM Static and MM Dynamic) given for a 25 year-old subject, MR models were characterized. Analytical solutions for uniform biaxial deformation were compared with the experimental biaxial data given in [7] to validate the quasi-static MR models. Finally, the MR material models for HA41 and MM Static were implemented in LS-DYNA (ver.970) and the model results were compared with the experimental oscillatory biaxial data.

Fluid-Structure Interaction

A simplified FE model of aorta (Figure 2a) was developed based on the geometry and dimension from a human aorta used in the biaxial tests [10]. The aortic wall was modeled with one-layer solid elements. Four approaches were used to model the fluid namely, Lagrangian, Eulerian, Arbitrary Lagrangian-Eulerian (ALE), and Smoothed Particle Hydrodynamics (SPH). In the Lagrangian method, the mesh is attached to the body and it transforms according to the deformation of the material. The Eulerian approach is solving the problem with a fixed mesh in space through which the material flows. Therefore, some initially void elements, representing the environment, are needed. In the ALE approach, in each time step, a Lagrangian material deformation is considered followed by an advection for fluid calculations. In the SPH formulation, the fluid is represented by particles which interact with one another and the surroundings through specific potential energy functions. Computations were performed using LS-DYNA (ver. 970) for the Lagrangian, Eulerian and ALE models, and PAM-CRASH (ver. 2002) for the SPH model.

To perform the pressurization simulation, particularly for the ALE and SPH models, a reservoir tube and a piston were used to create the fluid inflow boundary condition at the inlet of the tube. A linear ramp representative of cadaveric sled tests was taken as the pressure input (Figure 2b). The model was symmetric with respect to the X-Y plane and fixed boundary conditions (no flow) were defined at the other end. For fluid-structure interaction (FSI) in LS-DYNA, coupling of the Lagrangian mesh of aorta with the Eulerian mesh of the fluid was used. For this purpose in PAM-CRASH, the node to segment contact was implemented. A friction coefficient of 0.08 was assumed in the ALE and the SPH model between fluid and structure, which created flow characteristics consistent with the Eulerian model.

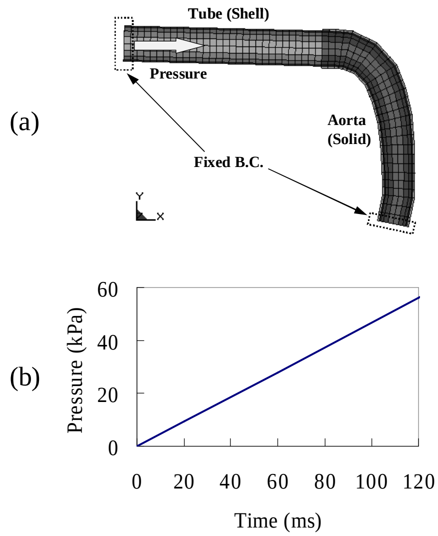

Figure 2. Simplified FE aorta model and pressure history

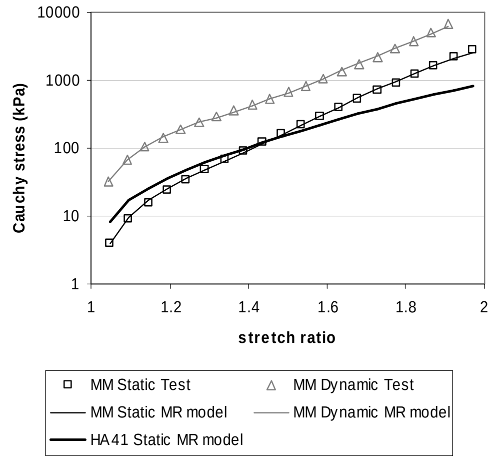

Figure 3. Responses to uniaxial loading. Experimental and MR model results for the quasi-static and dynamic tests of MM, and FE model results for the HA41 sample

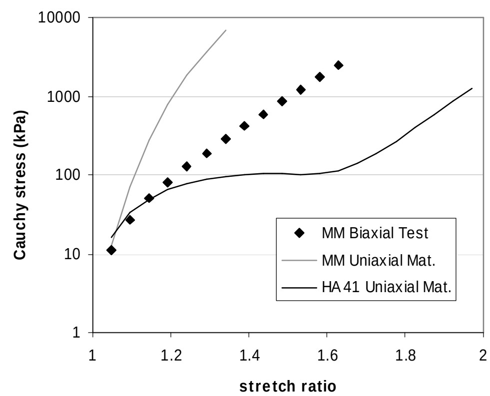

Figure 4. Responses to uniform biaxial loading. Experimental and MR model results for the quasi-static test of MM and MR model results for the HA41 sample

RESULTS AND DISCUSSION

The material parameters determined for the MM Static, MM Dynamic, and HA41 models are summarized in Table 1. For HA41, the experimental strains were all below 40%. Therefore, any result of this model for higher strains is merely speculative. The MR material model was able to closely match the uniaxial MM Static and MM Dynamic data (Figure 3). The behavior of the model for HA41, which was characterized based on the biaxial oscillatory results, in uniaxial deformation, was close to the MM Static data particularly at strains below 40%. In uniform biaxial deformation (Figure 4), the response of the MM Static model was significantly stiffer than the reported biaxial data. However, the response of the HA41 model, at strains below 40% was closer to the experimental biaxial data.

Table 1.
Material properties (in kPa) of the MR models for the quasi-static and dynamic results of Mohan and Melvin and the hyperelastic response of the biaxial test of HA41

Test	MM Static	MM Dynamic	HA41
C_{10}	1.16E+01	1.67E+02	1.96E+01
C_{01}	7.17E-01	-4.83E+01	9.25E+00
C_{11}	-2.64E+03	-3.82E+03	-5.73E+01
C_{20}	1.06E+03	1.81E+03	5.46E+01
C_{02}	1.71E+03	2.00E+03	1.41E+01

FE simulation of the oscillatory biaxial deformation with HA41 model showed that forces and strains were closely following the experimental data (Figure 5 and Figure 6 respectively). The stiffness hourglass coefficient (type 4) for this simulation was HG=0.1 and the ratio of hourglass energy to internal energy was less than 5%. The fact that E22 in the experiment was larger than the model showed that the tissue was anisotropic. For the FE simulation with MM Static material model, with HG=0.1 the ratio of hourglass energy was 40% and the forces were significantly higher than the experimental data. With HG=0.001, the forces were close to the experimental data, but the strains were low and excessive deformation occurred in the boundary (Figure 6). Therefore, the MM Static and biaxial data led to contradictory uniaxial and biaxial responses. The HA41 material properties closely described the experimental data for strains below 40%.

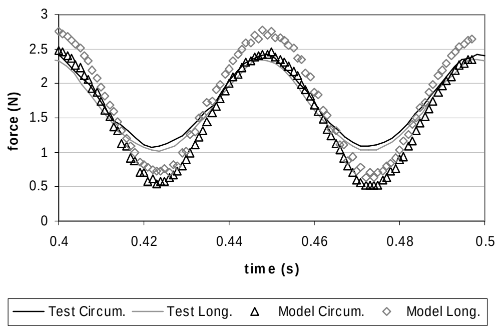

Figure 5. Comparison of forces in the circumferential and longitudinal directions between biaxial test data and FE results with HA41 MR material model

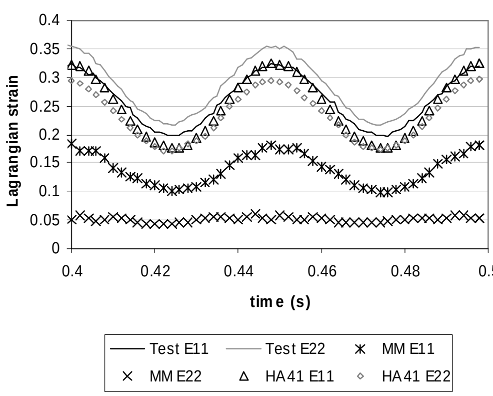

Figure 6. Comparison of strains between biaxial test data and FE results with MM static and HA41 MR material models

Based on the material parameters of HA41, the FSI models were used to simulate the *in vitro* pressure tests described in [10]. The velocity profile and pressure distribution in the fluid were considered as the main factors representing the flow characteristics which were measured at the isthmus region. Although all approaches predicted a parabolic velocity profile which is expected for Poiseuille-like flows, the Lagrangian method showed excessive mesh distortion which caused rapid drop of the time-step during simulation (Figure 7). All three FSI models predicted generation of vortices at the isthmus only when the loading rate was increased to 20 kPa/ms. For the test loading condition (0.5 kPa/ms) no vortices occurred. The maximum velocity was in the range of 2.5 to 3.0 mm/ms at 120ms. The pressure distribution was uniformly decreasing along the tube with about 60% of the input pressure at the isthmus.

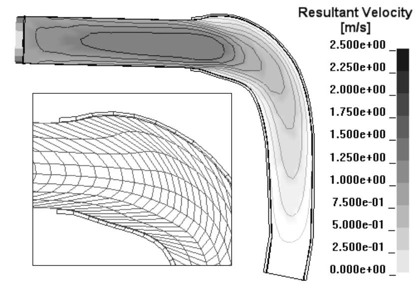

(a) Lagrangian fluid

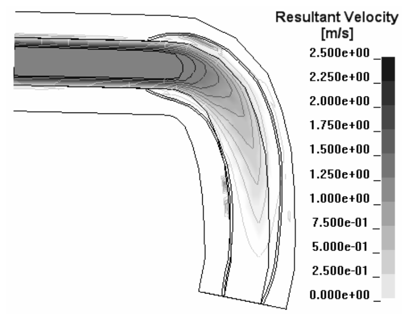

(b) Eulerian fluid

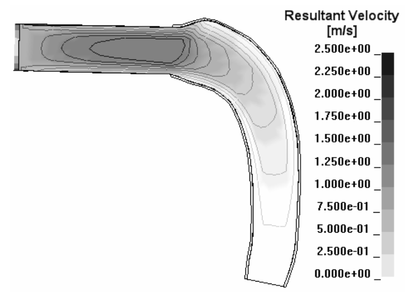

(c) ALE fluid

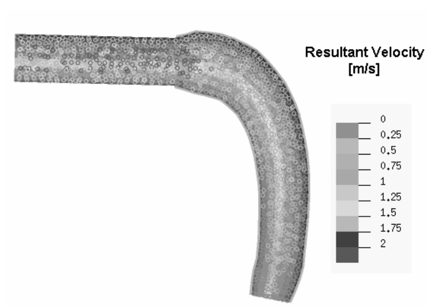

(d) SPH fluid

Figure 7. Comparison of velocity profiles of FSI models (at 100ms)

The trend of stretch ratios and stresses measured in the circumferential and longitudinal directions were consistent in the three FSI models. However, the results of the SPH model were higher than the two other models (Figure 9). In the SPH model, the identical material model was not used as only the first-order Mooney-Rivlin was available in the PAM-CRASH solver and it resulted in slightly different behavior. In the ALE model, the flow could not propagate as much as in the Eulerian and SPH models and the deformation of aorta was more concentrated in the ascending region. The maximum principal stress was predicted at the inner arch of the wall, close to the isthmus, in the range of 250 to 275kPa in the circumferential direction (Figure 8). The results were compared with the uniaxial failure tests [6] and the pressurization tests [10] (Figure 10). The material models used in this study were characterized based on sub-failure deformations (maximum strain about 15%). As a result, the stress-stretch ratio curves predicted from the models were almost linear and did not show the nonlinear trend observed in the experiments in large stretch ratios. However, the maximum values of stress and strain were located within the experimental data range. Neither in LS-DYNA nor in PAM-CRASH there is a material model that can handle both the nonlinearity and anisotropy that is observed in the aorta tissue. In the Eulerian method, because of the void elements, the total number of elements was higher than the others and also required the largest CPU calculation time (Table 2). For the SPH approach, the initial time step was the largest and the CPU time was the smallest in this simulation. However, as the number of elements grows, calculation time may increase dramatically.

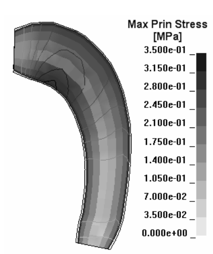

(a) Eulerian

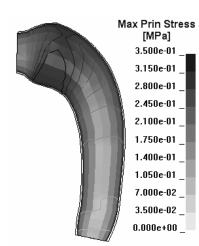

(b) ALE

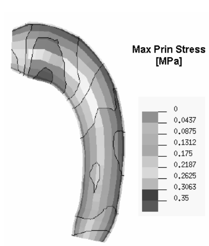

(c) SPH

Figure 8. Maximum principle stress distribution

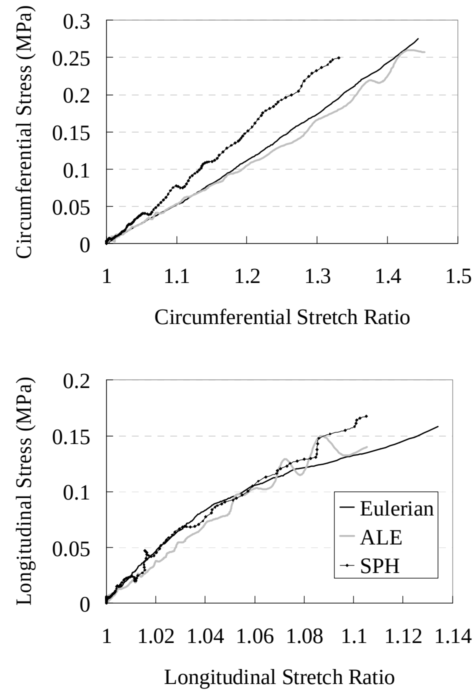

Figure 9. Aorta wall stress-stretch ratio at isthmus

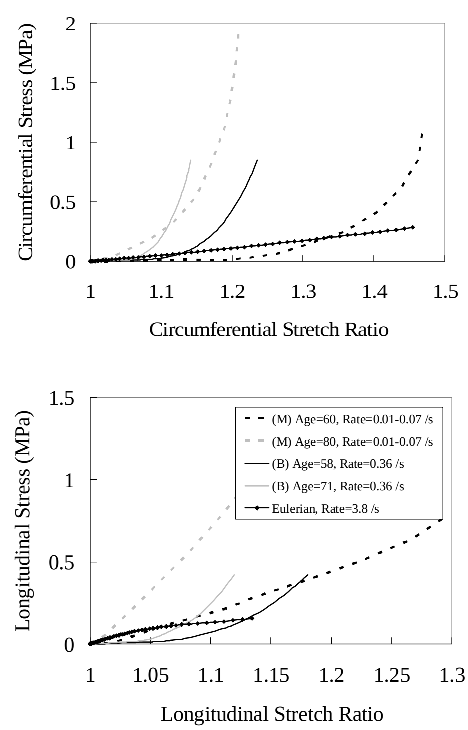

Figure 10. Stress vs. stretch ratio at isthmus and comparison with experiments

Table 2.
Computational aspects of the models

Element formulation	Eulerian	ALE	SPH
Elements	6544	1904	2016
Δt_i (μsec)	0.97	0.97	1.75
CPU time (sec)	11238	5626	3940
Solver	LS-DYNA	LS-DYNA	PAM-CRASH
CPU Clock	Intel® Pentium®4 2.8GHz		

CONCLUSIONS

Three TRA models with material properties determined from dynamic biaxial tests were validated against *in vitro* tests and predicted the most probable location of rupture at the isthmus as indicated in the experiments. The Eulerian approach was the most complete one in terms of including the flow and interaction with the wall, though it required relatively large computational time. The ALE approach resulted in less flow and more localized deformation in the aorta. The SPH approach exhibited rather idealized behavior of the fluid flow but the results in the aorta wall were close to the Eulerian approach with less computational time.

REFERENCES

[1] Katyal, D., McLellan, B.A., Brenneman, F.D., Boulanger, B.R., Sharkey, P.W., Waddell, J.P. 1997. "Lateral impact motor vehicle collisions: significant cause of blunt traumatic rupture of the thoracic aorta." J. Trauma, No. 42 (5): 769-772.

[2] Richens, D., Field, M., K., Neale, M., Oakley, C. 2002. "The mechanism of injury in blunt traumatic rupture of the aorta." Eur. J. Cardiothorac Surg., No. 21: 288-293.

[3] Lundewall, J. 1964. "The mechanics of traumatic rupture of the aorta." Acta. Pathol. Microbiol. Scand., No. 62: 34-36.

[4] Crass, J. R., Cohen, A.M., Motta, A.O., Tomashefski, J.F., Wiesen, E.J. 1990. "A proposed new mechanism of traumatic aortic rupture: the osseous pinch." Radiology, No. 176: 645-649.

[5] Symbas, P. N., Tyres, D.H., Ware, R.E. 1973. "Traumatic rupture of the aorta." Ann. Surg., No. 178 (6).

[6] Mohan, D., Melvin, J.W. 1982. "Failure properties of passive human aortic tissue I-Uniaxial tension tests." J. Biomechanics, No. 15 (11): 887-902.

[7] Mohan, D., Melvin, J.W. 1983. "Failure properties of passive human aortic tissue II-Biaxial tension tests." J. Biomechanics, No. 16 (1): 31-44.

[8] Shah, C. S., Yang, K.H., Hardy, W., Wang, H.K., King, A. 2001. "Development of a computer model to predict aortic rupture due to impact loading." Stapp Car Crash Journal, No. 45.

[9] Richens, D., Mark, F., Shahrul, H., Michael, N., Charles, O. 2004. "A finite element model of blunt traumatic aortic rupture." Eur. J. Cardiothorac Surg.

[10] Bass, C. R., Darvish, K., Bush, B., Crandall, J.R. 2001. "Material properties for modeling traumatic aortic rupture." Stapp Car Crash Journal, No. 45.

[11] Hallquist, J. O. 1998. "LS-Dyna Theoretical Manual."